

EMBEDDED INTER-SUBJECT VARIABILITY IN ADVERSARIAL LEARNING FOR INERTIAL SENSOR-BASED HUMAN ACTIVITY RECOGNITION

Francisco M. Calatrava-Nicolás^{1,*} Shoko Miyauchi^{1,†} Vitor Fortes Rey^{3,4} Paul Lukowicz^{3,4}
Todor Stoyanov¹ Oscar Martinez Mozos⁵

¹ Centre for Applied Autonomous Sensor Systems (AASS), Örebro University, Örebro, Sweden

² Faculty of Information Science & Electrical Engineering, Kyushu University, Fukuoka, Japan

³ RPTU, Kaiserslautern, Germany

⁴ DFKI, Kaiserslautern, Germany

⁵ Escuela Técnica Superior de Ingeniería y Diseño Industrial, Universidad Politécnica de Madrid, Madrid, Spain

ABSTRACT

This paper addresses the problem of Human Activity Recognition (HAR) using data from wearable inertial sensors. An important challenge in HAR is the model's generalization capabilities to new unseen individuals due to inter-subject variability, i.e., the same activity is performed differently by different individuals. To address this problem, we propose a novel deep adversarial framework that integrates the concept of inter-subject variability in the adversarial task, thereby encouraging subject-invariant feature representations and enhancing the classification performance in the HAR problem. Our approach outperforms previous methods in three well-established HAR datasets using a leave-one-subject-out (LOSO) cross-validation. Further results indicate that our proposed adversarial task effectively reduces inter-subject variability among different users in the feature space, and it outperforms adversarial tasks from previous works when integrated into our framework. Code: <https://github.com/FranciscoCalatrava/EmbeddedSubjectVariability>. git

Index Terms— Human Activity Recognition, Inertial Wearable Sensors, Inter-Subject Variability, Deep Adversarial Learning

*First Author - francisco.calatrava-nicolas@oru.se

†Corresponding Author - miyauchi@irvs.ait.kyushu-u.ac.jp

Francisco M. Calatrava-Nicolas and Todor Stoyanov gratefully acknowledge financial support from the Wallenberg AI, Autonomous Systems and Software Program (WASP) under the Knut and Alice Wallenberg Foundation. Computations were carried out on resources provided by the National Academic Infrastructure for Supercomputing in Sweden (NAISS), partially funded by the Swedish Research Council (grant no. 2022-06725).

Vitor Fortes Rey and Pau Lukowicz also thank the Carl Zeiss Stiftung, Germany, for support through its Sustainable Embedded AI project (P2021-02-009) and the Cross-Act project (01IW25001).

This is the accepted manuscript. The final published article is available at <https://doi.org/10.1109/MLSP62443.2025.11204225>

© 2025 IEEE. Personal use of this material is permitted. Permission from IEEE must be obtained for all other uses, in any current or future media, including reprinting/republishing this material for advertising or promotional purposes, creating new collective works, for resale or redistribution to servers or lists, or reuse of any copyrighted component of this work in other works.

1. INTRODUCTION

The problem of human activity recognition (HAR) consists of identifying the activities carried out by a person by analyzing the data collected with different sensors [1]. HAR is applied in different research areas, such as healthcare and well-being monitoring [2], human-robot interaction (HRI) [3], or autonomous vehicles [4].

This paper focuses on the application of HAR to classify activities using data from wearable inertial sensors. Although this problem has been lately addressed using different deep learning approaches [5, 6, 7, 8, 9, 10, 11], it still presents some challenges. A key issue, and the main focus of this paper, is to reduce the generalization gap when applying the method to previously unseen users. This gap arises from the heterogeneity in data distributions due to inter-subject variability, i.e., different individuals perform the same activity differently. In particular, individuals perform the same activity with varying levels of intensity and speed, influenced by factors such as personal preferences and physical characteristics. The resulting sensor-signal variations are often complex and non-linear, posing a challenge for accurate activity recognition [12]. This problem could be addressed by collecting and annotating extensive volumes of activity data to capture the diversity of real-world situations, however, it would require extra effort and resources. Therefore, it is desirable to design models that focus on learning features that generalize well among different individuals [13]. Thus, recent research has focused on reducing data distribution shifts among users to enhance classification performance without requiring additional data collection. In this context, different representation learning approaches including multitask, adversarial, and self-supervised learning have been proposed [8, 9, 10, 11].

These works still present some limitations. For example, [9] presents a multi-task learning framework that combines activity and user recognition, raising concerns related to privacy and scalability. Some methods attempt to address these privacy and generalization issues using adversarial learning, typically by introducing a user specific discrimination task within the adversarial framework [10, 8]. However, these strategies often struggle to ensure consistent generalization over all users like in [10], or they suffer from scalability constraints like in [8]. A more detailed discussion of previous methods and their limitations is provided in Section 2.

To address these limitations while narrowing the generalization gap, we propose a new adversarial learning framework that integrates the concept of inter-subject variability. We devise a novel adversarial task that determines whether a pair of activity feature vectors comes from the *same* person and the *same* activity, or from *different* persons but still the *same* activity. Our key insight is that embedding the activity together with the user dimension within the discrimination task will facilitate finding a common deep feature space for the same activity while intrinsically reducing the inter-subject variability for that activity, which helps close the generalization gap to unseen individuals. In addition, we frame our discrimination task as a binary classification problem, which does not increase the number of classes in the discriminator component with the number of users and thus enhances the scalability of our method. Moreover, we propose a novel combined loss function that integrates the non-saturating GAN loss function to learn subject-invariant feature representations. Finally, the adversarial nature of our framework may reduce privacy concerns [14]. We evaluate our framework using a Leave-One-Subject-Out (LOSO) cross-validation setup in three well-established datasets (PAMAP2, MHEALTH, REALD-ISP) in the HAR field, ensuring that in each iteration of the cross-validation, the model is tested on data from a previously unseen individual. LOSO is supported by previous works [15, 6] as an effective method for simulating real-world conditions.

In summary, our contributions are: (i) A novel deep adversarial framework that embeds the concept of inter-subject variability. (ii) Novel combined loss function to learn subject-invariant features. (iii) LOSO cross-validation comparison with state-of-the-art methods in three well-established datasets. (iv) Further ablation studies demonstrating the performance of our framework.

2. RELATED WORK

The activity recognition problem using wearable inertial sensors has been addressed using different deep learning methods. Convolutional neural networks (CNNs) have been used to classify windowed sensor signals as one-shot inputs [6, 7], sometimes with attention mechanisms [16]. Recurrent models (RNN) like LSTM[17] or hybrid models such as CNLSTM [18] have been applied as well, showing good results. Multi-task learning has also been adopted to enhance performance across related tasks. For example, [9] combines activity and user recognition in a multi-task setting. However, the complexity of the user classifier increases with the addition of new participants, raising concerns about scalability. Moreover, their use of cross-validation does not guarantee user-level separation for training and test sets, potentially leading to information leakage and an overestimation of the model’s ability to generalize to new users. In addition, [9] trains a user recognition network, which may lead to potential privacy issues [14]. Recently, adversarial networks have been proposed to improve the HAR problem. These methods try to find a common feature space that generalizes among different users. This is achieved through an adversarial user-based discrimination task that guides the learning process towards less user-discriminant feature space that may reduce privacy concerns [14] and improve generalization. For example, [10] trains the discriminator to tell whether two feature vectors come from the same user, while simultaneously pushing the feature extractor to remove personal cues so that the discriminator can no longer tell them apart. However, to get these feature vectors, it samples user pairs randomly, which could hurt the uniform representation over all the users. [8] improves this by assigning a unique class to each participant, achieving better generalization. However, the user classifier also grows in complexity

with the addition of new participants. Finally, the approach in [11] introduces self-supervised auxiliary tasks combining diversity generation and contrastive learning. While effective, their framework requires fine-tuning per test participant and uses a modified LOSO protocol, limiting comparability. In contrast to the previous works, we propose a new adversarial framework that integrates a new discrimination task that takes into account the inter-person variability for the same activity. In particular, our discrimination task is framed as a binary classification problem that does not scale with the number of participants as in [8]. Furthermore, and compared to [10], we included the activity information in the discrimination task, proposing a tailored organization of the original dataset for this novel discrimination task. Finally, our approach integrates a feature extractor with a reduced parameter count [6] to promote computational efficiency while preserving sufficient representational capacity.

3. ADVERSARIAL LEARNING FRAMEWORK FOR INTER-SUBJECT VARIABILITY REDUCTION

Our input set consist of signals from c uni-dimensional sensor channels, segmented with a sliding window of size w . We write it as $X = \{x_i\}_{i=1}^M \mid x_i \in R^{w \times c}$, where M is the number of input data samples in the dataset. We then define our labeled input dataset for the activity recognition task as:

$$A = \{x_i, y_i, s_i\}_{i=1}^M \mid y_i \in Y, s_i \in S \quad (1)$$

where $Y = \{y_1, \dots, y_K\}$ represents the set of K activity labels to be recognized, and S is the set of subject. To integrate the concept of inter-subject variability, we define a new input set A' for our discrimination task.

$$A' = \{(x_a, x_b)_i^y, (s_a, s_b)_i, g_i\}_{i=1}^N \mid x_a, x_b \in X, x_a \neq x_b, y \in Y, s_a, s_b \in S, g_i \in G = \{0, 1\} \quad (2)$$

where $(x_a, x_b)_i^y$ represent two different data samples $x_a, x_b \in X$ that share the same activity label $y \in Y$; (s_a, s_b) are two subjects from which the corresponding data samples (x_a, x_b) are selected. Finally, $g_i \in G$ is a binary label with value 1 if data samples x_a and x_b belong to the same subject, i.e. $s_a = s_b$, or value 0 if they belong to different subjects, i.e. $s_a \neq s_b$. The idea behind A' is to account for the fact that different individuals may perform the same activity in different ways. Our main insight is that embedding the activity label into the adversarial task encourages the model to learn a shared feature space for each activity, which in turn reduces the influence of inter-subject variability. The size of A' grows with the number of combinations of activities and subjects. To keep a manageable size, we uniformly sample the same number of data instances per class in G .

We define four blocks in our framework: the feature extractor F , the reconstructor R , the activity classifier C , and the discriminator D . The architecture details for each module are provided in [19]. The full framework is depicted in Fig. 1. The feature extractor encodes the input sensor data \mathcal{X} into a lower dimensional latent space \mathcal{L} , i.e. $F : \mathcal{X} \rightarrow \mathcal{L}$. The objective of F is to learn a latent feature space that, while fooling the discriminator, remains effective for the activity classification task. In this work, we use the network from [6] without its classification layer. The reconstructor R decodes the latent space \mathcal{L} into the original input space \mathcal{X} , i.e. $R : \mathcal{L} \rightarrow \mathcal{X}$. This block stabilizes the adversarial training [20]. We use the mean square error function for the reconstruction loss:

$$L_R = \|R(F(x_i)) - x_i\|_2^2 \quad (3)$$

where x_i is the input inertial signal (cf. Eq. 1).

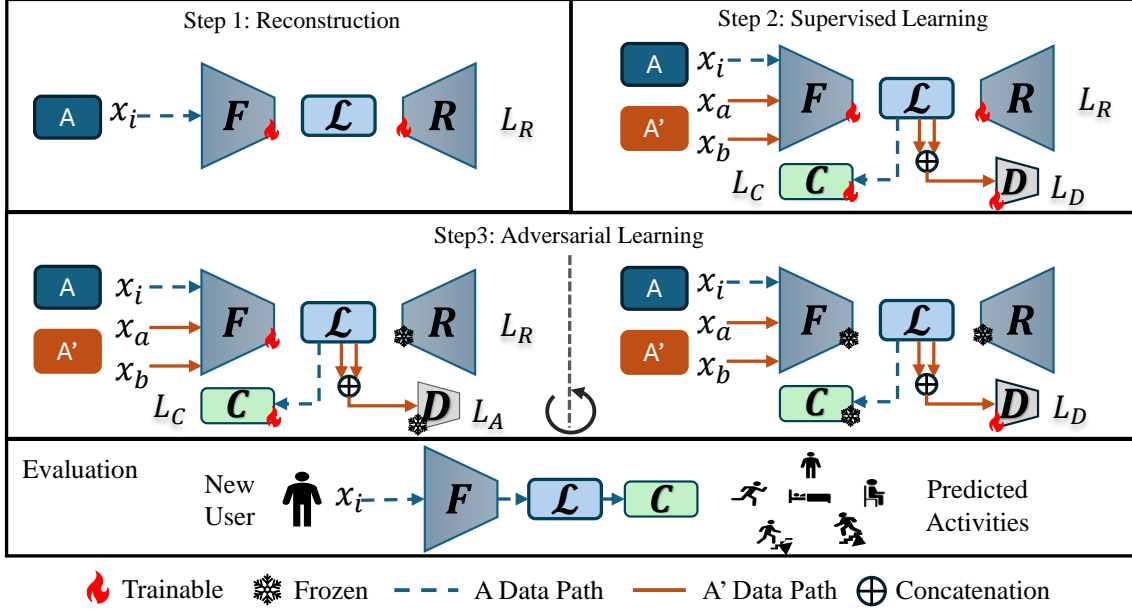


Fig. 1: Overview of our framework: Steps 1–2 pre-train all module weights. Step 3 introduces adversarial learning to minimize inter-subject variability. Evaluation is performed on previously unseen users. Data distribution A is used for the activity classification (Eq. 1), while A' is the data distribution used in the adversarial task (Eq. 2). The circular arrow in Step 3 illustrates the iterative nature of adversarial learning.

The activity classifier C maps the latent space \mathcal{L} into the activities space \mathcal{Y} , i.e., $C : \mathcal{L} \rightarrow \mathcal{Y}$. We use cross-entropy loss for the activity classification loss:

$$L_C = - \sum_{j=1}^{|\mathcal{Y}|} z_j \log C(F(x_i))_j \quad (4)$$

where z is a binary vector of size $|\mathcal{Y}|$ whose component $z_j = 1$ if the original activity label for x_i is y_j or zero otherwise.

Lastly, our binary discriminator D maps the latent space \mathcal{L} into our activity-based binary discriminative classes \mathcal{G} , i.e., $D : \mathcal{L} \rightarrow \mathcal{G}$. D takes as input the concatenated feature vectors of each pair drawn from A' . We use binary cross-entropy as the discrimination loss:

$$L_D = -g_i \log D((F(x_a) \oplus F(x_b))_i) - (1-g_i) \log 1 - D((F(x_a) \oplus F(x_b))_i) \quad (5)$$

where x_a and x_b represent the two data samples comprising the i_{th} pair, g_i corresponds to the label of the i_{th} pair (cf. Eq. 2), and \oplus represents the concatenation.

Drawing inspiration from [8], our training process is divided into three steps. The first two steps focus on pre-training the weights of the feature extractor F , the reconstructor R , the activity classifier C , and the discriminator D . The third step incorporates the adversarial learning. Specifically, in step 1, we train F and R using the reconstruction loss L_R on samples drawn from A (Eq. 1).

In step 2, we train F , R , C , and D simultaneously in a supervised way. In this step, R and D are optimized by minimizing L_R and L_D , respectively, using data from A' (Eq. 2). Additionally, C is trained by minimizing L_C on data from A . Finally, F is updated by minimizing both L_R and L_C , using data from A and A' . We define the combined loss function for F during step 2 as:

$$L_F^{\text{step2}}(\theta_F; A, A') = L_C(\theta_F; A) + L_R(\theta_F; A') \quad (6)$$

where θ_F denotes the parameters of the feature extractor F .

The step 3 implements the deep adversarial learning process. Inspired by the adversarial training paradigm in GANs [21], this third step is further subdivided into two sub-steps that are repeated iteratively. In the Step 3.1, F is trained by minimizing a combined loss function consisting of L_R , L_C , and the adversarial loss L_A (Eq. 8) over data distributions A and A' , while the weights of D and R are frozen. The combined loss function for F in this step is:

$$L_F^{\text{step3.1}}(\theta_F; A, A') = w_A L_A(\theta_F; A') + w_R L_R(\theta_F; A') + w_C L_C(\theta_F; A) \quad (7)$$

where w_A , w_R , and w_C are scalar weights that balance the adversarial, reconstruction, and classification objectives, respectively, and L_A is the non-saturating loss [21]. This novel combined loss unifies the adversarial, reconstruction, and classification terms, allowing F to learn feature representations that preserve classification performance while fooling the discriminator. L_A is defined as follow:

$$L_A = -\log D((F(x_a) \oplus F(x_b))_i), \forall \{(x_a, x_b)_i, g_i\} \in A' | g_i = 0 \quad (8)$$

where x_a, x_b represent the two data samples comprising the i_{th} pair, g_i corresponds to the label of the i_{th} pair (cf. Eq. 2), and \oplus represents the concatenation operation. In Step 3.2, D is trained by minimizing L_D (Eq. 5) using A' as input set, while the parameters of F, R , and C remain frozen. This alternating optimization allows F to learn latent feature representations that confuse D (Step 3.1), while D learns to distinguish them (Step 3.2), driving the adversarial learning. The intuition behind using the non-saturating adversarial loss (Eq. 8) is to train the feature extractor F to produce representations of data from different individuals, i.e., $g = 0$ (Eq. 2), that, in the eyes of the discriminator D , seem to come from the same subject. For that, the pair of feature vectors coming from a different user ($g = 0$) are labeled as coming from the same subject ($g = 1$). In this way, the feature extractor is pushed to remove subject-specific cues. The full training process is depicted in Algorithm 1.

Algorithm 1 Training algorithm for our framework

1: for $epoch = 1$ to $Epoch_{step1}$ do	▷ Step 1
2: for each $batch$ in X_A from A do	
3: $\theta_F \leftarrow \theta_F - \alpha_F \nabla_{\theta_F} L_R(\theta_F; X_A)$	▷ Eq. 3
4: $\theta_R \leftarrow \theta_R - \alpha_R \nabla_{\theta_R} L_R(\theta_R; X_A)$	
5: for $epoch = 1$ to $Epoch_{step2}$ do	▷ Step 2
6: for each $batch$ in A and A' do	
7: $\theta_F \leftarrow \theta_F - \alpha_F \nabla_{\theta_F} L_F^{step2}(\theta_F; X_A, X_{A'})$	▷ Eq. 6
8: $\theta_R \leftarrow \theta_R - \alpha_R \nabla_{\theta_R} L_R(\theta_R; X_{A'})$	
9: $\theta_C \leftarrow \theta_C - \alpha_C \nabla_{\theta_C} L_C(\theta_C; X_A)$	▷ Eq. 4
10: $\theta_D \leftarrow \theta_D - \alpha_D \nabla_{\theta_D} L_D(\theta_D; X_{A'})$	▷ Eq. 5
11: We freeze R	
12: for $epoch = 1$ to $Epoch_{step3}$ do	▷ Step 3
13: for each $batch$ in A and A' do	
14: We freeze D (Step 3.1)	
15: $\theta_F \leftarrow \theta_F - \alpha_F \nabla_{\theta_F} L_F^{step3.1}(\theta_F; X_A, X_{A'})$	▷ Eq. 7
16: $\theta_C \leftarrow \theta_C - \alpha_C \nabla_{\theta_C} L_C(\theta_C; X_A)$	
17: We unfreeze D and we freeze F and C (Step 3.2)	
18: $\theta_D \leftarrow \theta_D - \alpha_D \nabla_{\theta_D} L_D(\theta_D; X_{A'})$	

4. DATASETS AND SETUP

We apply our method to three HAR datasets: PAMAP2 [22], MHEALTH [23], and REALDISP [24]. PAMAP2 [22] contains 54 sensor cues from 9 subjects performing 18 (12 from a protocol + 6 extra) activities. They provided inertial signals from 3 IMUs (worn on the dominant wrist, chest, and dominant leg). For classification, we use the 3D acceleration ($\pm 16g$) and gyroscope data corresponding to the 12 protocol activities, excluding data from the ninth subject due to insufficient samples. We segment the data using a 512-sample sliding window with a 50% overlap. MHEALTH [23] comprises 12 activities from 10 participants with sensors on the chest, right wrist, and left ankle; we use the 3D acceleration and gyroscope segmented with a 512-sample window and a 50% overlap. REALDISP [24] includes 33 activities from 17 participants using 9 sensors placed on various body parts; we use the accelerometer and gyroscope signals (54 signals total) and segment the data using a 256-sample sliding window with a 50% overlap. Across all datasets, windows spanning multiple labels are discarded.

Following [15, 6], we apply LOSO cross validation, which consists of testing the model on one different user in each iteration, while training in the remaining set of users. In this way, test users remain unseen until evaluation. In addition, we designate two users from the training as the validation set to monitor the overfitting during training. All datasets are normalized via min-max scaling using parameters from the training sets. Each experiment is repeated twice with different random seeds, and the results are averaged. We compare our approach with prior works on the HAR field using wearable inertial sensors, in particular, MCCNN [7], DCLSTM [18], METIER [9], UIDFE [8], and DDLearn [11]. Note that while the original UIDFE method [8] incorporates unlabeled test data during training, we modify it to exclude any test data. Additionally, unlike DDLearn [11]—which uses only 20% of left-out testing participants—we evaluate on 100% of the test subjects. We implemented the methods from [7, 18, 9, 8] according to their original descriptions, while for [11], we used the publicly provided code. All experiments were run in Python 3.10.12 using PyTorch 2.2.0 on Ubuntu 18.04, running on NVIDIA Quadro RTX 6000 and NVIDIA Tesla A40 GPUs. In Step 1, modules F and R are trained with a learning rate of 10^{-4} for 20 epochs. Step 2 trains the same modules plus C

Table 1: Comparison with previous approaches (Best in bold).

Dataset	Model	Accuracy	$F1 - Score_M$
PAMAP2	MCCNN	0.7939 \pm 0.0770	0.7511 \pm 0.0940
	DCLSTM	0.7853 \pm 0.1012	0.7266 \pm 0.1113
	METIER	0.7924 \pm 0.0597	0.7540 \pm 0.0574
	UIDFE	0.8014 \pm 0.1353	0.7648 \pm 0.1447
	DDLearn	0.7188 \pm 0.1561	0.6442 \pm 0.1691
	Ours	0.8703 \pm 0.1219	0.8643 \pm 0.1431
REALDISP	MCCNN	0.8378 \pm 0.0601	0.6651 \pm 0.0998
	DCLSTM	0.9420 \pm 0.0497	0.9094 \pm 0.0627
	METIER	0.9177 \pm 0.0567	0.8099 \pm 0.1080
	UIDFE	0.9450 \pm 0.0670	0.9283 \pm 0.0700
	DDLearn	0.8476 \pm 0.0902	0.7802 \pm 0.1323
	Ours	0.9710 \pm 0.0423	0.9651 \pm 0.0368
MHEALTH	MCCNN	0.8736 \pm 0.0739	0.7888 \pm 0.0823
	DCLSTM	0.8482 \pm 0.1051	0.8157 \pm 0.1169
	METIER	0.8583 \pm 0.0746	0.8252 \pm 0.0932
	UIDFE	0.8982 \pm 0.0667	0.8275 \pm 0.0881
	DDLearn	0.8529 \pm 0.0684	0.7825 \pm 0.0764
	Ours	0.9225 \pm 0.0606	0.9065 \pm 0.0780

and D for 10 epochs, with a learning rate of 10^{-4} for all except C , which uses 10^{-5} . Finally, Step 3 further refines F , C , and D for 150 epochs at a learning rate of 10^{-4} for all except F , which uses 10^{-3} . We used Adam as optimizer. The values for the weights $w_R=0.7$, $w_C=0.2$, and $w_A=0.1$ in Eq. 7 were found via grid search. All experiments were carried out under consistent hyperparameter settings and preprocessing conditions (cf. Sec. 4). Moreover, the set A' was resized to ensure an balanced number of samples for both classes in G : PAMAP2 and REALDISP contained 25,000 per class, and MHEALTH contained 5,000 per class (cf. Sec.3). The batch size for the A set was 64 for step 1 and 32 for step 2 and 3. The batch sizes for A' were adjusted to keep an equal number of batches with A .

5. EXPERIMENTAL RESULTS

In this section, we first compare our proposed method with previous works in the HAR field. We then conduct a distribution distance-based study, showing that our method reduces data shifts between train and test distributions. In addition, we provide an ablation study to measure the impact of each component in our framework. We also introduce a discrimination task study to compare discrimination tasks from previous works in our proposed framework. Finally, we provide a hyperparameter study for the weights in Eq. 7.

First, we compare our method against previous works [7, 18, 9, 8, 11] (Sec. 4) using both Accuracy and F1-Score Macro ($F1 - Score_M$). As shown in Table 1, our method outperforms all previous works under the same preprocessing conditions. Fig. 2 (left column) further illustrates the distribution of F1-Score Macro using box plots. Notably, our method yields the lowest Interquartile Range (IQR) in 2 of the 3 datasets, indicating reduced variability. In addition, our minimum score surpasses every other method’s lower bound across all datasets. Together, these findings suggest that our framework narrows the generalization gap and demonstrates stronger robustness, outperforming previous methods under a LOSO cross-validation setup.

Next, we explore the reduction of the inter-person variability when applying our approach. Specifically, we show that our adversarial task reduces the distribution distance for the same activity between training and testing participants. Our premise is that this reduction may facilitate the recognition of activities in new unseen

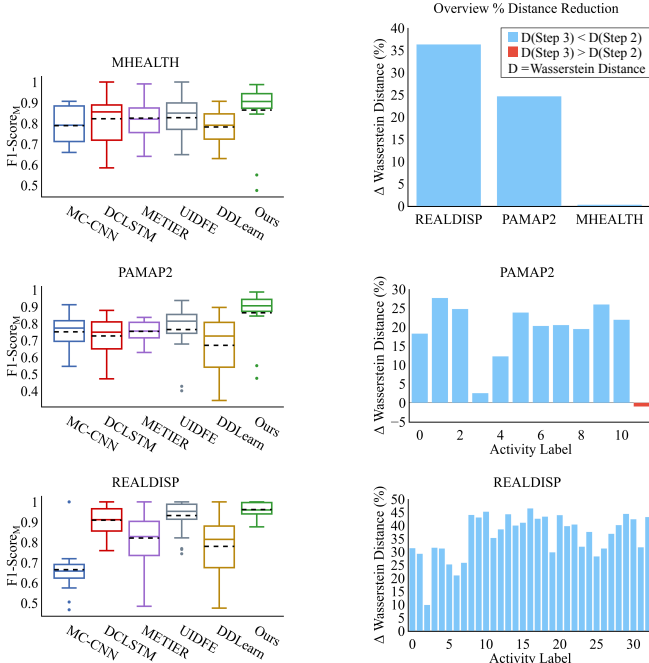


Fig. 2: First column: $F1 - Score_M$ for MHEALTH, PAMAP2, and REALDISP (top-down). Second column: Percentage change in Wasserstein distance from Step 2 to Step 3 between training and test set distributions. The top plot gives the distance change per dataset, while the middle (PAMAP2) and bottom (REALDISP) plots detail the distance change per activity. Positive bars (blue) mark a reduction (distance after Step 3 is smaller than after Step 2); negative bars (red) mark an increase.

persons. To study this reduction, firstly, we measure the distribution distance for the same activity between the training and the left-out testing participant after Step 2 (Sec. 3) and then we average over all left-out testing participants in the LOSO. Secondly, we repeat the same procedure after Step 3, which is the adversarial step. Finally, we compare both distances. We use the Wasserstein distance [25] to measure the distribution distances. This comparison is done to study the effect of our adversarial task on the reduction of the inter-person variability for each activity. Results are shown in Figure 2 (right column). In these plots, bars show the percentage change in Wasserstein distance from Step 2 to Step 3, expressed relative to the Step 2 distance. A positive bar means the distance decreased (distance after Step 3 is smaller than after Step 2), while a negative bar means it increased. The top plot in Figure 2 provides an overview of the decrease in Wasserstein distance from Step 2 to Step 3 per dataset. The results indicate a notable decrease in distance for the PAMAP2 and REALDISP datasets. This suggests that Step 3, which is the adversarial step, effectively reduces the discrepancy between training and testing distributions. For the MHEALTH dataset, the distance is marginally reduced, implying that the method has a limited impact in this case. These findings are in accordance with the results in Table 2 (ablation study), which show greater improvements from Step 2 to Step 3 for PAMAP2 and REALDISP. The center and lower plots of Figure 2 (right column) show specific results by activity for the PAMAP2 and REALDISP datasets, respectively. Across both plots, distances after Step 3 are lower than after Step 2 for every activity, except for one PAMAP2 case where the distance increase is under 1%. This indicates that our adversarial discrimination task effectively

Table 2: Ablation Study (Best in bold).

Dataset	Disc	Accuracy	$F1 - Score_M$
PAMAP2	Superv	0.7472 ± 0.1067	0.7444 ± 0.1232
	Step 2	0.8179 ± 0.1255	0.8229 ± 0.1357
	Ours	0.8703 ± 0.1219	0.8643 ± 0.1431
REALDISP	Superv	0.9064 ± 0.0724	0.9220 ± 0.0566
	Step 2	0.9372 ± 0.0512	0.9098 ± 0.0620
	Ours	0.9710 ± 0.0423	0.9651 ± 0.0368
MHEALTH	Superv	0.9014 ± 0.0633	0.8934 ± 0.0718
	Step 2	0.9121 ± 0.0707	0.8880 ± 0.0891
	Ours	0.9225 ± 0.0606	0.9065 ± 0.0780

Table 3: Comparison to prior discrimination tasks (Best in bold).

Dataset	Disc	Accuracy	$F1 - Score_M$
PAMAP2	D_i	0.8274 ± 0.1045	0.7869 ± 0.1102
	D_b	0.8130 ± 0.1453	0.7636 ± 0.1579
	Ours	0.8703 ± 0.1219	0.8643 ± 0.1431
REALDISP	D_i	0.9447 ± 0.0772	0.9394 ± 0.0566
	D_b	0.9511 ± 0.0619	0.9445 ± 0.0538
	Ours	0.9710 ± 0.0423	0.9651 ± 0.0368
MHEALTH	D_i	0.9173 ± 0.0698	0.8892 ± 0.0938
	D_b	0.9225 ± 0.0707	0.9010 ± 0.0867
	Ours	0.9225 ± 0.0622	0.9065 ± 0.0801

reduces the inter-person variability for the same activities. We omit detailed results for the MHEALTH dataset since the per-activity distances after Step 2 and Step 3 were very similar, resulting in the overall improvement shown in Figure 2 (right column, top).

Following that, we present the ablation study of our framework. We compare three variants of our framework: one that trains F together with a classification layer in an end-to-end supervised way as in [6]. Another that considers supervised learning together with reconstruction (essentially we stop training at step 2 in Algorithm 1). Finally, the third step presents the results of our full approach. The comparison results are shown in Table 2. By comparing results across these three experiments, we can assess how the reconstructor and the adversarial learning process each contribute to the final improved performance of our framework. Across all datasets, our proposed method consistently outperforms both baselines. These results suggest that the proposed adversarial step enhances the model’s generalization capabilities.

One of the main contributions of this paper is the discrimination task that integrates the concept of inter-person variability (Sec. 3). To test its performance, we compare it to the discrimination tasks previously presented in [8] and [10]. To this end, we keep the same F , R , and C , and we change the discriminator D accordingly to the discrimination tasks. We first implement a discriminator, D_i , that tries to identify each particular user as proposed in [8]. The second implemented discriminator, D_b , takes as input two feature vectors and decides whether they belong to the same participant, as proposed in [10]. The third discriminator is our proposed task. Comparison results are shown in Table 3, where our discrimination task achieves the best classification results across all datasets. Moreover, it provides the smallest deviation for MHEALTH and REALDISP, and the second lowest for PAMAP2.

Finally, we investigate the influence of the three weights w_R , w_C , and w_A in the combined loss function from Eq. 7 on the activity classification performance. The evaluation is based on the average classification accuracy and $F1 - Score_M$ obtained from the LOSO

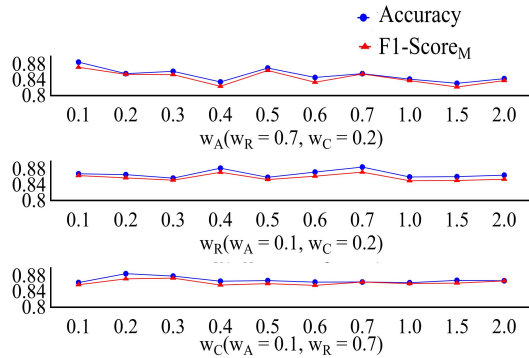


Fig. 3: Average accuracy and $F1 - Score_M$ for variations in w_A (top), w_R (middle), and w_C (bottom) for PAMAP2.

benchmark when varying the range of a single weight while keeping the other two weights fixed. Two weights are held constant at the values determined through an initial grid search, as outlined in Section 4, while the remaining weight is incrementally varied across a predefined range. Each data point presented in Figure 3 corresponds to the mean classification accuracy obtained for a specific combination of the three weight values. Figure 3 shows that, when each weight is varied independently, the accuracy fluctuates by less than 1–2% across the full range of values, indicating the model is largely insensitive to moderate shifts. Overall, this highlights that our framework is robust to the choice of hyperparameter.

6. CONCLUSIONS

We presented a new adversarial deep learning framework for the problem of human activity recognition based on wearable inertial sensor data. Based on the concept of inter-subject variability, we designed a new discrimination task that takes into account information about the activity label together with the subject dimension, with the purpose of finding a common latent feature space for the same activity among different subjects to reduce their distribution distances. We conducted extensive experiments on three distinct HAR datasets, using LOSO cross-validation to assess our proposed framework performance across unseen subjects. The results show that our framework consistently outperforms existing state-of-the-art methods, highlighting its superior ability to generalize across different individuals. Furthermore, we performed comparative analyses against previously proposed discrimination tasks within adversarial learning paradigms in the HAR problem showing that our discrimination task improves the classification results when integrated into the adversarial framework. We also show evidence on the reduction of the inter-subject variability gap for the same activity between different users underscoring the potential of our approach to facilitate the development of more adaptable and user-agnostic HAR systems.

7. REFERENCES

- [1] Jose M Chaquet, Enrique J Carmona, and Antonio Fernández-Caballero, “A survey of video datasets for human action and activity recognition,” *Computer Vision and Image Understanding*, vol. 117, no. 6, pp. 633–659, 2013.
- [2] Christian Debes, Andreas Merentitis, Sergey Sukhanov, Maria Niessen, Nikolaos Frangiadakis, and Alexander Bauer, “Monitoring activities of daily living in smart homes: Understanding human behavior,” *IEEE Signal Process. Mag.*, vol. 33, no. 2, pp. 81–94, 2016.
- [3] Lasitha Piyathilaka and Sarath Kodagoda, “Human activity recognition for domestic robots,” in *Field and Service Robotics: Results of the 9th International Conference*. Springer, 2015, pp. 395–408.
- [4] Eshed Ohn-Bar and Mohan Manubhai Trivedi, “Looking at humans in the age of self-driving and highly automated vehicles,” *IEEE T. Intell. Veh.*, vol. 1, no. 1, pp. 90–104, 2016.
- [5] Tiago Fernandes Tavares and Lucas Bertoloto, “Air drums, and bass: Anticipating musical gestures in accelerometer signals with a lightweight cnn,” in *IEEE International Workshop on Machine Learning for Signal Processing*, 2023, pp. 1–5.
- [6] Francisco M. Calatrava-Nicolás and Oscar Martínez Mozos, “Light residual network for human activity recognition using wearable sensor data,” *IEEE Sensors Letters*, vol. 7, no. 10, pp. 1–4, 2023.
- [7] Jianbo Yang, Minh Nhut Nguyen, Phyo Phyo San, Xiaoli Li, and Shonali Krishnaswamy, “Deep convolutional neural networks on multichannel time series for human activity recognition,” in *International Joint Conference on Artificial Intelligence*, 2015, vol. 15, pp. 3995–4001.
- [8] Sungho Suh, Vitor Fortes Rey, and Paul Lukowicz, “Adversarial deep feature extraction network for user independent human activity recognition,” in *IEEE International Conference on Pervasive Computing and Communications*, 2022, pp. 217–226.
- [9] Ling Chen, Yi Zhang, and Liangying Peng, “Metier: A deep multi-task learning based activity and user recognition model using wearable sensors,” *Proceedings of the ACM on Interactive, Mobile, Wearable and Ubiquitous Technologies*, vol. 4, no. 1, pp. 1–18, 2020.
- [10] Lei Bai, Lina Yao, Xianzhi Wang, Salil S Kanhere, Bin Guo, and Zhiwen Yu, “Adversarial multi-view networks for activity recognition,” *Proceedings of the ACM on Interactive, Mobile, Wearable and Ubiquitous Technologies*, vol. 4, no. 2, pp. 1–22, 2020.
- [11] Xin Qin, Jindong Wang, Shuo Ma, Wang Lu, Yongchun Zhu, Xing Xie, and Yiqiang Chen, “Generalizable low-resource activity recognition with diverse and discriminative representation learning,” in *ACM SIGKDD Conference on Knowledge Discovery and Data Mining*, 2023, pp. 1943–1953.
- [12] Billur Barshan and Aras Yurtman, “Investigating inter-subject and inter-activity variations in activity recognition using wearable motion sensors,” *The Computer Journal*, vol. 59, no. 9, pp. 1345–1362, 2016.
- [13] Thomas Plötz, “If only we had more data!: Sensor-based human activity recognition in challenging scenarios,” in *IEEE International Conference on Pervasive Computing and Communications Workshops*, 2023, pp. 565–570.
- [14] Yusuke Iwasawa, Kotaro Nakayama, Ikuko Yairi, and Yutaka Matsuo, “Privacy issues regarding the application of dnns to activity-recognition using wearables and its countermeasures by use of adversarial training,” in *International Joint Conference on Artificial Intelligence*, 2017, pp. 1930–1936.
- [15] Nils Y Hammerla and Thomas Plötz, “Let’s (not) stick together: pairwise similarity biases cross-validation in activity recognition,” in *ACM international joint conference on pervasive and ubiquitous computing*, 2015, pp. 1041–1051.

- [16] Yang Wang, Hongji Xu, Yunxia Liu, Mengmeng Wang, Yuhao Wang, Yang Yang, Shuang Zhou, Jiaqi Zeng, Jie Xu, Shijie Li, and Jianjun Li, “A novel deep multi-feature extraction framework based on attention mechanism using wearable sensor data for human activity recognition,” *IEEE Sensors Journal*, vol. 23, no. 7, pp. 7188–7198, 2023.
- [17] Fabio Hernández, Luis F. Suárez, Javier Villamizar, and Miguel Altuve, “Human activity recognition on smartphones using a bidirectional lstm network,” in *Symposium on image, signal processing and artificial vision*, 2019, pp. 1–5.
- [18] Francisco J. Ordóñez and Daniel Roggen, “Deep convolutional and lstm recurrent neural networks for multimodal wearable activity recognition,” *Sensors*, vol. 16, no. 1, pp. 115, 2016.
- [19] Francisco M. Calatrava-Nicolás, “Paper code,” <https://github.com/FranciscoCalatrava/EmbeddedSubjectVariability.git>.
- [20] Abu Zaher Md Faridee, Avijoy Chakma, Archan Misra, and Nirmalya Roy, “Strangan: Adversarially-learnt spatial transformer for scalable human activity recognition,” *Smart Health*, vol. 23, pp. 100226, 2022.
- [21] Ian Goodfellow, “Nips 2016 tutorial: Generative adversarial networks,” *arXiv preprint arXiv:1701.00160*, 2016.
- [22] Attila Reiss and Didier Stricker, “Introducing a new benchmarked dataset for activity monitoring,” in *International Symposium on Wearable Computers*, 2012, pp. 108–109.
- [23] Oresti Banos, Rafael Garcia, Juan A Holgado-Terriza, Miguel Damas, Hector Pomares, Ignacio Rojas, Alejandro Saez, and Claudia Villalonga, “mHealthDroid: a novel framework for agile development of mobile health applications,” in *International Work-Conference Ambient Assisted Living and Daily Activities*, 2014, pp. 91–98.
- [24] Oresti Banos, Mate Toth, and Oliver Amft, “REALDISP Activity Recognition Dataset,” UCI Machine Learning Repository, 2014, DOI: doi.org/10.24432/C5GP6D.
- [25] Charlie Frogner, Chiyuan Zhang, Hossein Mobahi, Mauricio Araya, and Tomaso A Poggio, “Learning with a wasserstein loss,” *Advances in neural information processing systems*, vol. 28, 2015.